Supplementary Information

A robust spectral reconstruction algorithm enables quantum dot spectrometers with subnanometer spectral accuracy

Spectral Reconstruction mathematical model:

This section describes how we acquire mathematical model of the computational spectrometer. After the incident light passes through the spatially distributed filters, intensity is modified to varying degrees at different wavelengths, and the resulting signals are captured by the camera. This process can be described mathematically as:

$$\int_{\lambda_{min}}^{\lambda_{max}} F(\lambda)R_i(\lambda)d\lambda = I_i \ (i = 1,2,3, \dots n) \tag{S1}$$

where I_i is the signal obtained at the pixel of the image sensor under the microfilter, i is the serial number of the microfilter, and $R_i(\lambda)$ generally represents the response spectrum of the pixel, which is obtained in the pre-calibration process and equals the product of transmittance of the QD microfilter and the inherent response spectrum of the image sensor. $F(\lambda)$ is the spectrum of the incident light to be reconstructed.

Before operating the spectrometer, one needs to take measurements to obtain the $R_i(\lambda)$, a process often referred to as the learning process, also known as the pre-calibration (or initialization) process. In the pre-calibration process, a spatially uniform monochromatic light is input and the corresponding signal of the pixel under each microfilter is collected. The wavelength of the monochromatic light is scanned at a given interval in the operating wavelength range to produce the $R_i(\lambda)$.

Considering that the output of a monochromator conforms to the Gaussian distribution,[45-46] a given spectrum can be decomposed based on the Gaussian basis. Therefore, we carried out the Gaussian basis-based decomposition of $F(\lambda)$:

$$F(\lambda) \approx \sum_{j=1}^{m} \phi_j(\lambda)x_j \tag{S2}$$

where $\phi_j(\lambda) = \frac{1}{\sigma\sqrt{2\pi}}\exp\left[-\frac{1}{2}\left(\frac{\lambda-\widehat{\lambda_j}}{\sigma}\right)^2\right]$, the parameter σ is defined as $\sigma = \left(2\sqrt{ln2}\right)^{-1}\delta_d$, where δ_d is half of the full width at half maximum (FWHM) of the actual monochromatic light. Here, $\widehat{\lambda_j}$ denotes the central wavelength of the monochromatic light for the j_{th} scan, and j represents the number of monochromatic lights involved in the scanning process, the scan resolution in short. At this point, the Eq. (S1) is rewritten as:

$$\sum_{j=1}^{m}\left(\int_{\lambda_{min}}^{\lambda_{max}} R_i(\lambda)\phi_j(\lambda)d\lambda\right) x_j = I_i(i = 1,2,3, \dots n) \tag{S3}$$

We set $A_{ij} = \int_{\lambda_{min}}^{\lambda_{max}} R_i(\lambda)\phi_j(\lambda)d\lambda$, and discretize the integration process, then the mathematical model

can be solved as the following matrix equation:

$$Ax = I \tag{S4}$$

At this point, the variable x to be solved is not the spectrum of the light to be measured, but the Gaussian base coefficient of the incident light. Due to the underdetermined character of the matrix A, it is not possible to obtain x by direct computation based on the inverse matrix. Therefore, as mentioned in the compressive sensing theory,[47-48] the solution of this problem is usually transformed into an optimization problem:

$$\begin{aligned} \min_{x} \ & \|Ax - I\|_{L_p} \\ & Ax = I \end{aligned} \tag{S5}$$

where L_p denotes the norm of the problem. Since the L_1 norm would constitute an NP-hard problem, the L_2 norm is normally used to formulate this problem.

Spectral Reconstruction Algorithm:

A number of works have chosen to use Tikhonov regularization, also known as the Ridge regression algorithm, to solve this problem, and the resulting mathematical model becomes：

$$\min_{x} \ L = \ \|Ax - I\|^2 + \gamma^2\|x\|^2 \tag{S6}$$

here, γ is the coefficient of the regular term and the pseudo-code for this algorithm is shown below:

Algorithm 1: Ridge regression

Input: $A,\ I,\ \gamma$;

Output:x;

1. $x = A^T I$;
2. $\gamma = \min_{\gamma} \frac{\|Ax-I\|_2^2}{\left[n-trace\left(A\left(AA^T+\gamma^2\right)^{-1}A^T\right)\right]^2}$;
3. $x = (A^T A + 2\gamma^2)^{-1}(A^T I)$;
4. **return** x;

We next add the TV regularization technique with AdaDelta iteration compared to the Ridge regression algorithm, which achieves a better broad spectrum response. Its mathematical model is:

$$\min_{x} \ L = \ \|Ax - I\|^2 + \gamma^2\|x\|^2 + \frac{\rho}{2}\|Gx\|^2 \tag{S7}$$

where γ and ρ are the coefficients of the corresponding regular terms, and G is the gradient computation matrix. The implementation details of Ridge+TV are shown in the pseudo-code below:

Algorithm 2: Ridge+TV

Input: $A,\ I,\ \gamma,\ \rho,\ \varepsilon,\ G$;

Output: x;

1. $x = A^T I$;
2. ***while***: $Gx \geq \varepsilon$;
3. $\Delta\hat{\gamma}_t = -\frac{\eta}{\sqrt{E[\gamma^2]_t+\varepsilon}}\gamma_t$;
4. γ=$\Delta\hat{\gamma}_t$+γ;
5. $x = (A^T A + \rho G^T G + 2\gamma^2)^{-1}(A^T I)$;
6. **return** x;

Subsequently, we further introduced ADMM to strengthen the control of the two canonical terms to achieve stronger anti-noise effect, and the obtained mathematical model is as follows：

$$\begin{gathered}\min_{x}\ L=\gamma^{2}\|x\|^{2}+\lambda\|y\|+\frac{\beta}{2}\left\|z-Ax+I+\frac{a}{\beta}\right\|+\frac{\alpha}{2}\left\|y-Gx+\frac{b}{\alpha}\right\| \\ s.t.\ \ z=Ax-I;\ y=Gx;\ \ Ax=I;\end{gathered} \tag{S8}$$

The pseudo-code for this algorithm is:

Algorithm 3: TKVA

Input: $A,\ I,\ \gamma,\ \varepsilon,\ G,\ a,\ \alpha,\ b,\ \beta,\ \lambda$;

Output: x;

1.$x=A^{T}I$;

2. ***while***: $y\geq\varepsilon$

3. **Update variables:**

4.. $x=(2\gamma^{2}I+\beta A^{T}A+\alpha G^{T}G)^{-1}\left(\beta A^{T}\left(z+b+\frac{a}{\beta}\right)+\alpha G^{T}\left(y+\frac{b}{\alpha}\right)\right)$;

5. $y=\max\left(|v_{2}|-\frac{\lambda}{\alpha},0\right)sign(v_{2})$, $v_{2}=Gx-\frac{b}{\alpha}$;

6. $z=\max(|v_{1}|,0)\,sign(v_{1})$, $v_{1}=Ax-I-\frac{a}{\beta}$;

7. **Update parameters:**

8. $a=a+\beta(z-Ax+I)$;

9. $b=b+\alpha(y-Gx)$;

10. $\alpha=\lambda\alpha$;

11. $\beta=\lambda\beta$;

12. $\Delta\hat{\gamma}_{t}=-\frac{\eta}{\sqrt{E[\gamma^{2}]_{t}+\varepsilon}}\gamma_{t}$;

13. $\gamma=\Delta\hat{\gamma}_{t}+\gamma$;

14. **return** x;

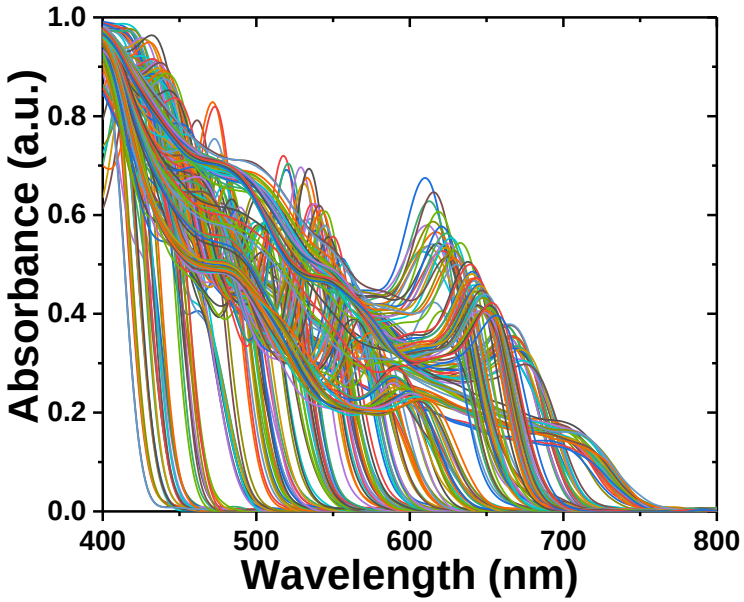

Fig. S1 Absorption spectra of all QDs used in this work.

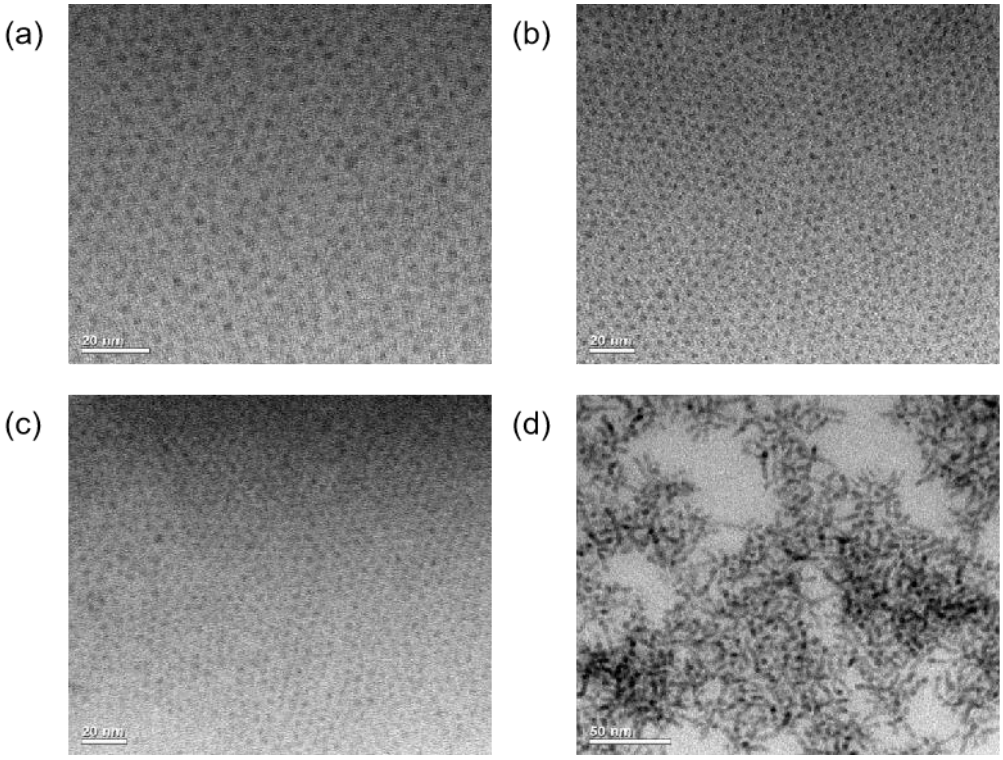

Fig. S2 Typical transmission electron microscope images of the four types of quantum dots: (a) CdS, (b) CdSxSe1-x, (c) CdSe, (d) CdTe.

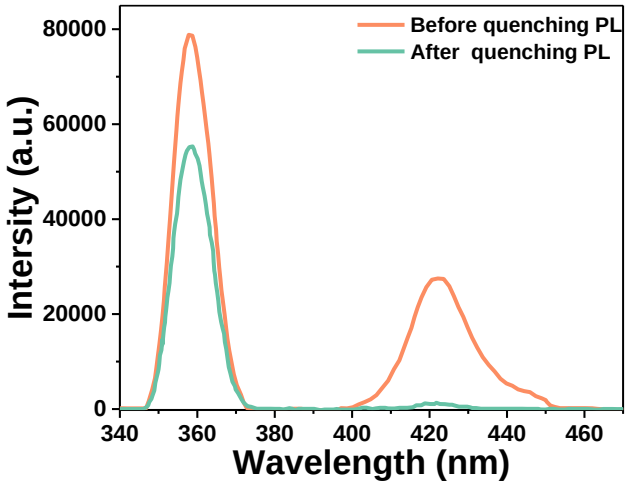

Fig. S3 Change of QD PL spectrum before and after introducing a fluorescence quencher.

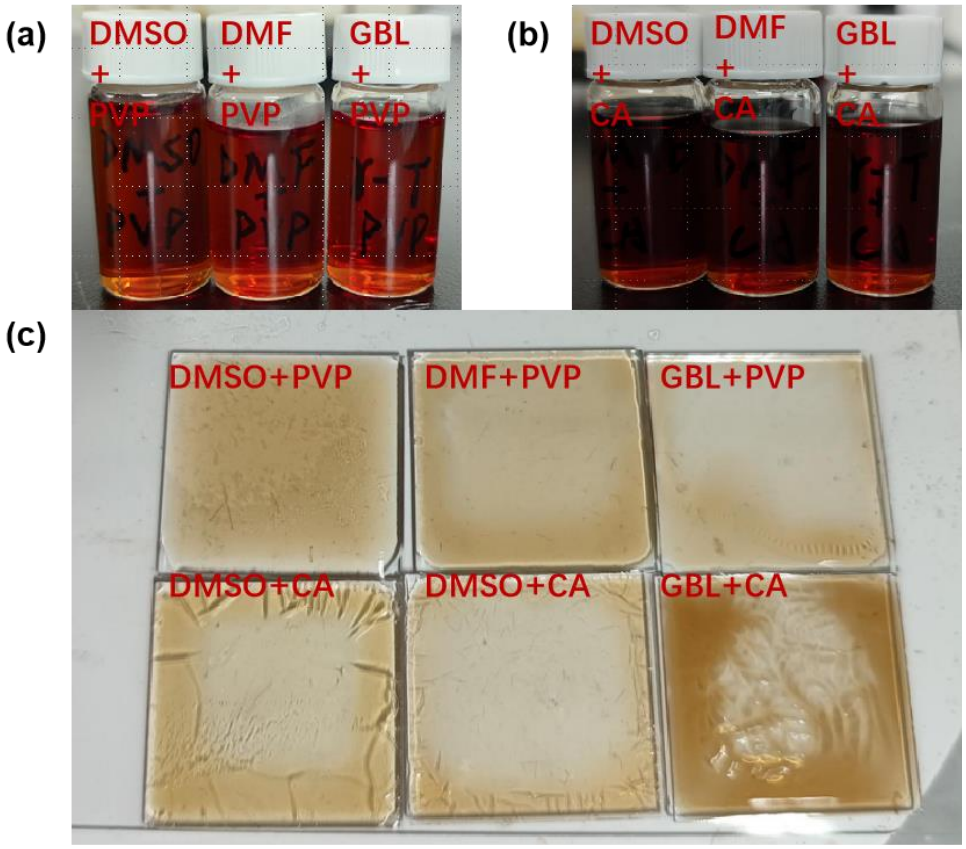

Fig. S4 Dispersion solutions of QDs after ligand exchange in different solvents and polymers systems. Two common polymers were selected: polyvinylpyrrolidone (PVP) and cellulose acetate (CA), along with three solvents: dimethyl sulfoxide (DMSO), dimethylformamide (DMF), and γ-butyrolactone (GBL). QD inks with equal concentrations were prepared and coated. (a) and (b) demonstrate good dispersion and stability of these QD inks. (c) shows the dispersion of QDs after film formation with the corresponding inks.

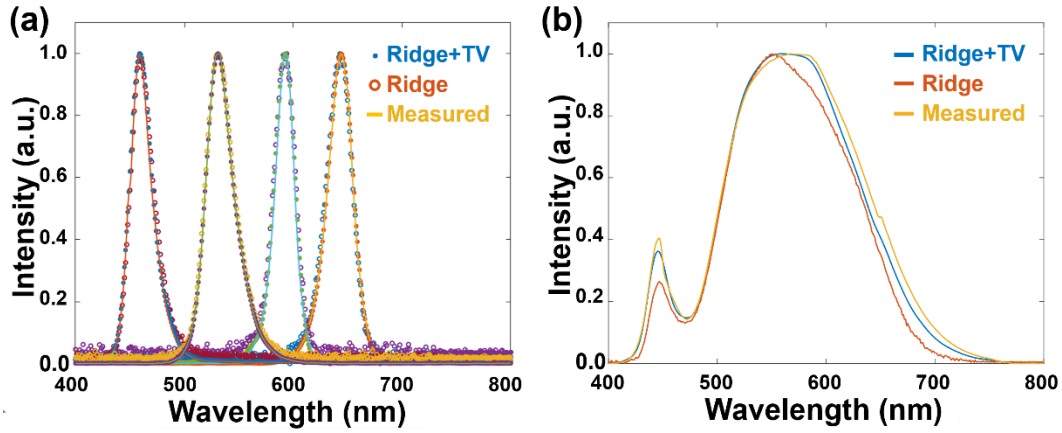

Fig. S5 a) Reconstruction results of monochromatic light using the Ridge+TV and Ridge regression algorithms. b) Recovery effect of Ridge+TV and Ridge regression algorithms for a white LED spectrum.

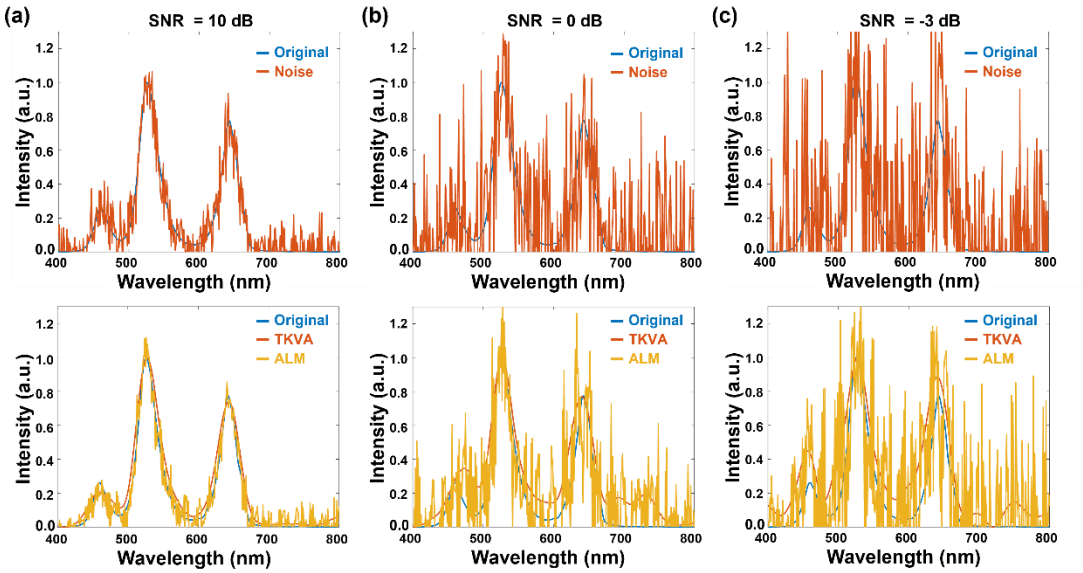

Fig. S6. Spectral reconstruction results of TKVA and ALM algorithms at noise level of: a) 10 dB, b) 0 dB, c) -3 dB.

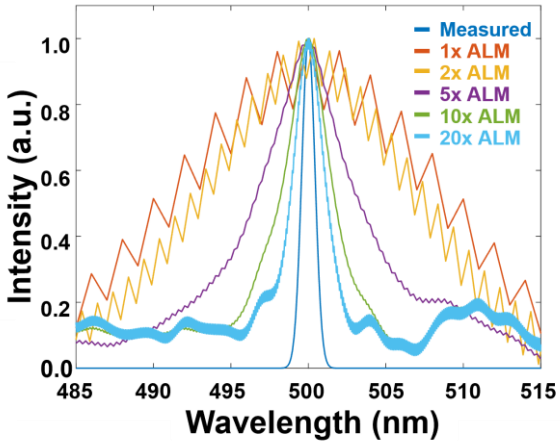

Fig. S7 Reconstruction results of the ALM algorithm at different interpolation factors.

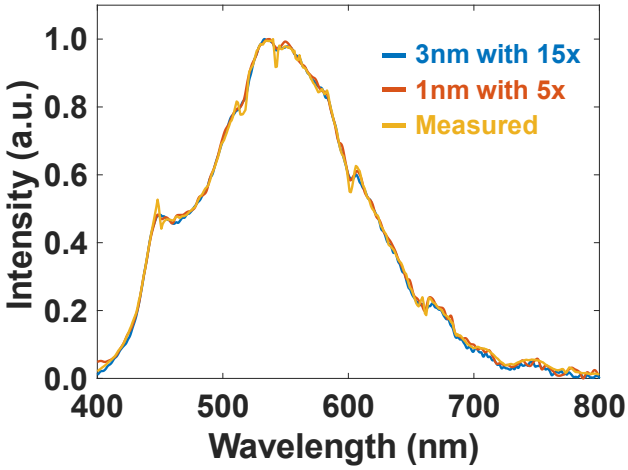

Fig. S8 Reconstruction results of TKVA algorithm with 15x interpolation for initialization data scanned every 3 nm and 5x interpolation scanned every 1 nm.

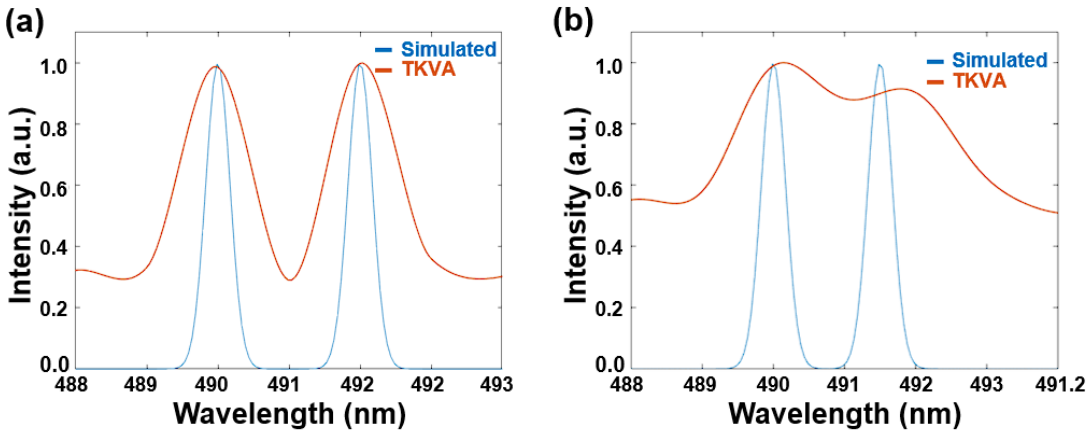

Fig. S9 Simulation results for spectral resolution according to the Rayleigh criterion. a) Two beams of monochromatic light separated by 2 nm, b) Two beams of monochromatic light separated by 1.6 nm.

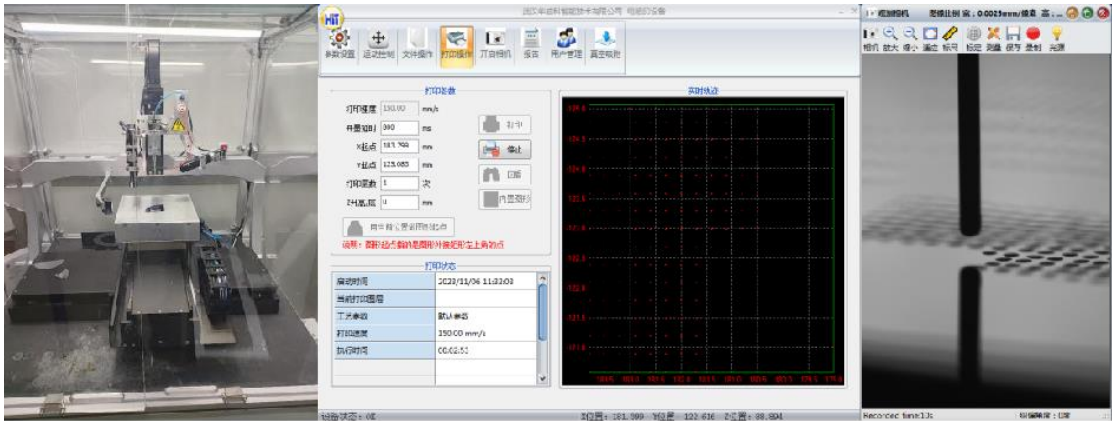

Fig. S10 The electrohydrodynamic jet printing equipment and its operating interface.